

**JUNIOR INDEPENDENT WORK, PART 2**  
**SPRING 2003**

ALEXEY SPIRIDONOV

This paper represents my own work in accordance with University regulations.

1. INTRODUCTION

**Definition 1.1.** A *sparse matrix* is a random symmetric matrix with independent entries  $a_{i,j}$ ,  $1 \leq i \leq j \leq n$ .  $a_{i,j}$  is 1 with probability  $\frac{\lambda}{n}$ , and 0 otherwise, where  $\lambda > 0$ .

**Definition 1.2.** A  $\pm$ -*sparse matrix* is a random symmetric matrix with independent entries  $a_{i,j}$ ,  $1 \leq i \leq j \leq n$ .  $a_{i,j}$  is 1 with probability  $\frac{\lambda}{2n}$ ,  $-1$  with probability  $\frac{\lambda}{2n}$ , and 0 otherwise, where  $\lambda > 0$ .

**Definition 1.3.** Let  $\nu_{a,b}(A)$  be the number of eigenvalues of  $A$  in the interval  $[a, b]$ .

Suppose  $A$  are random symmetric matrices with independent, identically distributed elements  $\frac{g}{\sqrt{n}}$ , where  $g$  is a Gaussian random variable, and  $n$  is the size of  $A$ . Then, a well known result [1] is that the variance,  $d\nu_{a,b}(A)$ , grows logarithmically with  $n$ .

On the other hand, the variance of  $n$  independent identically distributed (IID) random variables grows linearly with  $n$ .

Thus arises the question of whether  $d\nu_{a,b}(A)$  exhibits faster growth behaviors for types of random matrices other than those explored in [1].

Matrices with few non-zero elements (the colloquial sparse matrices) have long been of interest to mathematical physicists in modeling diverse types of systems [3]. They also have strong connections with questions in graph theory. Even letting these applications aside, the spectrum and the variability of eigenvalues of sparse and  $\pm$ -sparse matrices are interesting topics.

Their relevance to alternate patterns of growth of  $d\nu_{a,b}(A)$  is illustrated by the following heuristic argument. These kind of matrices have, on average,  $\lambda$  non-zero entries per row. When  $\lambda$  is relatively small, it is not unreasonable to expect the matrix to separate into components, order of  $n$  in quantity. So, the eigenvalues would be produced essentially as  $m$  IID variables, where  $m$  is of the order of  $n$ , and dependent upon  $\lambda$ . So, we may expect to see different growth rates of  $d\nu_{a,b}(A)$  than [1].

This paper presents a numerical investigation of the spectrum and the rate of growth of  $d\nu_{a,b}(A)$  of sparse and  $\pm$ -sparse matrices. We also show some preliminary steps towards deriving a density function for the eigenvalues of such matrices.

$\lambda$	0.2	0.5	0.7	0.9	1.0	1.2	1.5	1.7	1.9	20
$\pm$ -sparse	99.3	94.9	90.8	86.4	84.3	80.3	75.0	71.7	68.8	67.5
sparse	99.4	94.9	90.7	86.5	84.3	80.3	75.1	71.9	69.0	67.7

TABLE 1. Percentage of eigenvalues falling into  $[-1.5, 1.5]$ .

## 2. NUMERICAL RESULTS

We used the Intel Math Kernel Library (MKL) (see [2]) version of the Linear Algebra Package (LAPACK) [2] along with program in the C language.

We worked on estimates of the spectrum first, since they would assist us in choosing a suitable interval, on which to calculate  $\nu_{a,b}(A)$ . We chose a number of values of  $\lambda$  and  $n$  to show the trends in the spectra as a function of both variables. Due to time considerations, and since larger matrices provide more eigenvalues, we used 10000, 8000, 4000, 3000 and 2000 matrices for  $n = 10, 20, 50, 100$  and 200, respectively. The spectra are split into several figures for the sake of formatting. Figures 1 and 2 contain the results for  $\pm$ -sparse matrices with  $\lambda \leq 1$  and  $\lambda > 1$  respectively; Figures 3 and 4 contain analogous results for sparse matrices.

The spectra have a number of notable features. Not surprisingly, the spectra of sparse matrices are skewed to the right, growing more centered with  $n$  (see section 3);  $\pm$ -sparse ones are sign-symmetrical, and so are their spectra.

For smaller  $\lambda$  (sparser matrices), most of the weight falls on the “natural” eigenvalues 0 (primarily),  $\pm 1$ ,  $\pm\sqrt{2}$ ,  $\pm\frac{1\pm\sqrt{5}}{2}$ , and other simple quadratic expressions. That in itself is not very surprising — the explanation likely lies in the presence of many small subcomponents. However, it does warrant some formal investigation; it would also be interesting to explain the variation in the relative frequencies of those eigenvalues. The distributions are basically bimodal (discounting the spike at 0), but four or six subtler modes can be identified. All modes grow less pronounced with  $\lambda$  and  $n$ ; again, the explanation probably lies in the increase in frequency of more complex subcomponents that yield eigenvalues outside the fairly discrete positions given by smaller subcomponents; however, it is far less obvious how to formalize that intuition.

The plots show that the majority of the distribution lies in  $[-1.5, 1.5]$  in all cases; the percentage varies from 99% to 67%, depending on  $\lambda$ , see Table 1 for the details. We used a sample of 6000 matrices for each  $(n, \lambda)$  pair — hence, even when 99% of the spectrum is in the interval, the general trend is still detectable. As we shall see, this simplification of using a fixed interval (which is easily overcome) does not affect the quality of the results, and so is justified.

Having chosen  $[a, b]$ , we calculated  $\nu_{a,b}(A)$  for  $\pm$ -sparse and sparse matrices for a number of choices of  $(\lambda, n)$ , and estimated

$$(1) \quad d_{\lambda,n} = \frac{1}{n} \sum_{A; \lambda, n \text{ fixed}} \nu_{a,b}(A)^2 - \langle \nu_{a,b}(A) \rangle^2, \text{ where}$$

$$\langle \nu_{a,b}(A) \rangle = \frac{1}{n} \sum_A \nu_{a,b}(A)$$

Figures 6 and 7 show our results; it is clear that they are linear. We also present a subset of the data in Table 2 together with best-fit lines to the data with the  $r^2$ ,

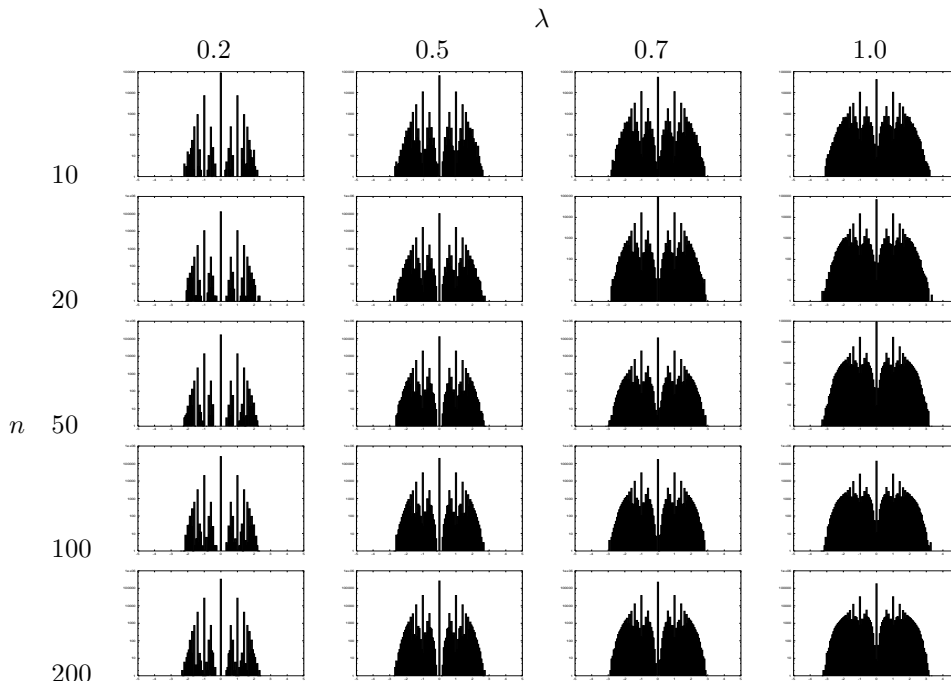


FIGURE 1. Approximations of spectra of  $\pm$ -sparse matrices for selected  $(\lambda, n)$ ,  $\lambda \leq 1$ : histograms of eigenvalues, plotted on a logarithmic scale. The  $x$ -axis scale is the same in all plots. The  $y$ -axis varies between 100,000 and  $10^6$ .

the squares of their Pearson correlation coefficients. The goodness of fit confirms that the trends are linear.

We additionally calculated  $\nu_{a,b}(A)$  for Gaussian matrices, also with a sample of 6000, and the same interval, which then contains  $\approx 86\%$  of the eigenvalues (as would be the case if the eigenvalues were Gaussian random variables:  $\int_{-1.5}^{1.5} \frac{e^{-\frac{x^2}{2}}}{\sqrt{2\pi}} \approx .86639$ ). The results are in Figure 5; the trend is logarithmic, rather than linear, which is in agreement with previous work [1]. This supports the validity of our numerical methods.

This is an exciting development, since it shows that the behavior of random matrices is more diverse than encompassed by current theories. Aside from motivating the development of exact descriptions of this behavior, our findings raise the question of the transition between the linear and logarithmic modes of growth; this change is visible in Figure 8 as  $\lambda$  grows. [3] shows for  $\pm$ -sparse matrices that with  $\lambda \rightarrow \infty$ , the spectrum of  $A$  approaches Wigner’s semicircular distribution with  $n \rightarrow \infty$ . This suggests that for high  $\lambda$  (the matrices no longer “sparse”) sparse matrices behave as the gaussian case.

### 3. PRELIMINARIES FOR FINDING EXACT SPECTRUM DENSITY

Ideally, we would like to show that all the moments of the eigenvalue distribution converge as  $n \rightarrow \infty$ , and, better yet, to find exact descriptions of them. In many

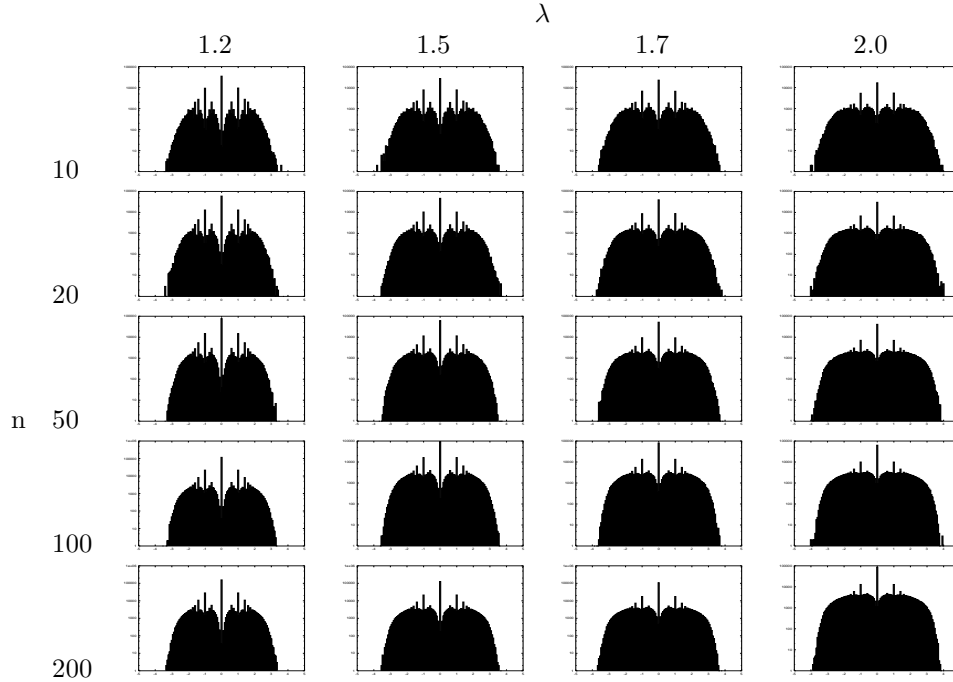


FIGURE 2. Approximations of spectra of  $\pm$ -sparse matrices for selected  $(\lambda, n)$ ,  $\lambda > 1$ . The axes are as in Figure 1.

		$\lambda$				
		0.2	0.7	1.0	1.5	2.0
$n$	5	0.043223	0.452320	0.652973	0.698664	0.596618
	10	0.113101	1.035600	1.365528	1.279780	1.087380
	15	0.186531	1.614398	2.014286	1.823147	1.617515
	20	0.213616	2.061573	2.729279	2.453276	2.057507
	25	0.297109	2.707664	3.490912	3.234313	2.561289
	35	0.434889	3.924578	4.496553	4.292098	3.503380
	50	0.569280	5.422053	6.611461	6.495984	5.252980
	75	0.940000	8.091557	10.362146	9.563120	7.081164
	100	1.331056	11.235226	12.949108	12.240471	10.296177
	$an$	$0.012697n$	$0.110234n$	$0.132643n$	$0.124963n$	$0.100809n$
$r^2$	0.99248	0.998775	0.997689	0.998479	0.99572	

TABLE 2. Values of  $d_{\lambda, n}$  in  $\pm$ -sparse matrices for a selection of  $(\lambda, n)$  pairs. For each value of  $\lambda$ , we also present the best-fit line  $d_{\lambda, n} = an$  and  $r^2$ .

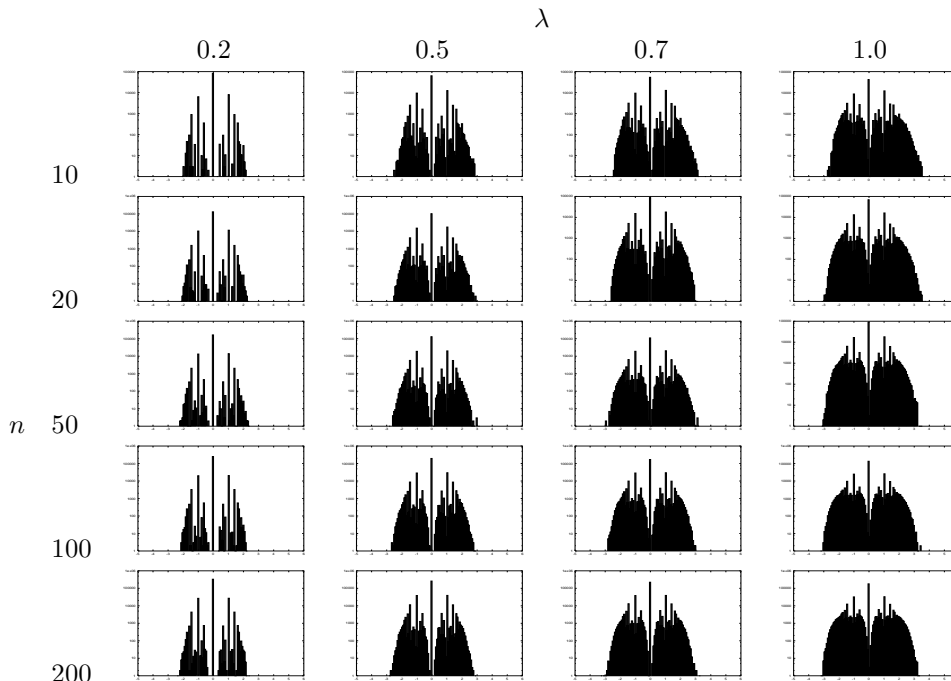


FIGURE 3. Approximations of spectra of sparse matrices for selected  $(\lambda, n)$ ,  $\lambda \leq 1$ . The axes are as in Figure 1.

ways, this task is similar to what Wigner’s proof accomplished; however, we do not have a conjecture of the density function — the spectral estimates suggest that the relationship between the limiting density and  $\lambda$  is subtle. Due to time constraints, we only present a few easy-to-calculate lower moments of sparse matrices.

$$\begin{aligned}
 (2) \quad \lim_{n \rightarrow \infty} \frac{1}{n} \langle \text{Tr } A \rangle &= \lim_{n \rightarrow \infty} \frac{1}{n} \langle \sum_{i=1}^n a_{ii} \rangle = \lim_{n \rightarrow \infty} \frac{1}{n} \sum_{i=1}^n \langle a_{ii} \rangle \\
 &= \lim_{n \rightarrow \infty} \frac{1}{n} \cdot \frac{\lambda}{n} \cdot n = 0
 \end{aligned}$$

$$\begin{aligned}
 (3) \quad \lim_{n \rightarrow \infty} \frac{1}{n} \langle \text{Tr } A^2 \rangle &= \lim_{n \rightarrow \infty} \frac{1}{n} \langle \sum_{i=1}^n \sum_{j=1}^n a_{ij} a_{ji} \rangle = \lim_{n \rightarrow \infty} \frac{1}{n} \sum_{i=1}^n \sum_{j=1}^n \langle a_{ij} \rangle \\
 &= \lim_{n \rightarrow \infty} \frac{1}{n} \cdot \frac{\lambda}{n} \cdot n^2 = \lambda
 \end{aligned}$$

$$(4) \quad \lim_{n \rightarrow \infty} \frac{1}{n} \langle \text{Tr } A^3 \rangle = \lim_{n \rightarrow \infty} \frac{1}{n} \langle \sum_{i=1}^n \sum_{j=1}^n \sum_{k=1}^n a_{ij} a_{jk} a_{ki} \rangle$$

In the case of  $A^3$ , there are several cases:

- (1) All indices  $i, j, k$  distinct; there are  $n(n-1)(n-2)$  such cases, and then  $\langle a_{ij} a_{jk} a_{ki} \rangle = \left(\frac{\lambda}{n}\right)^3$ , so the contribution of this cases:  $\lambda^3 \frac{n(n-1)(n-2)}{n^4} \rightarrow 0$  as  $n \rightarrow \infty$ .

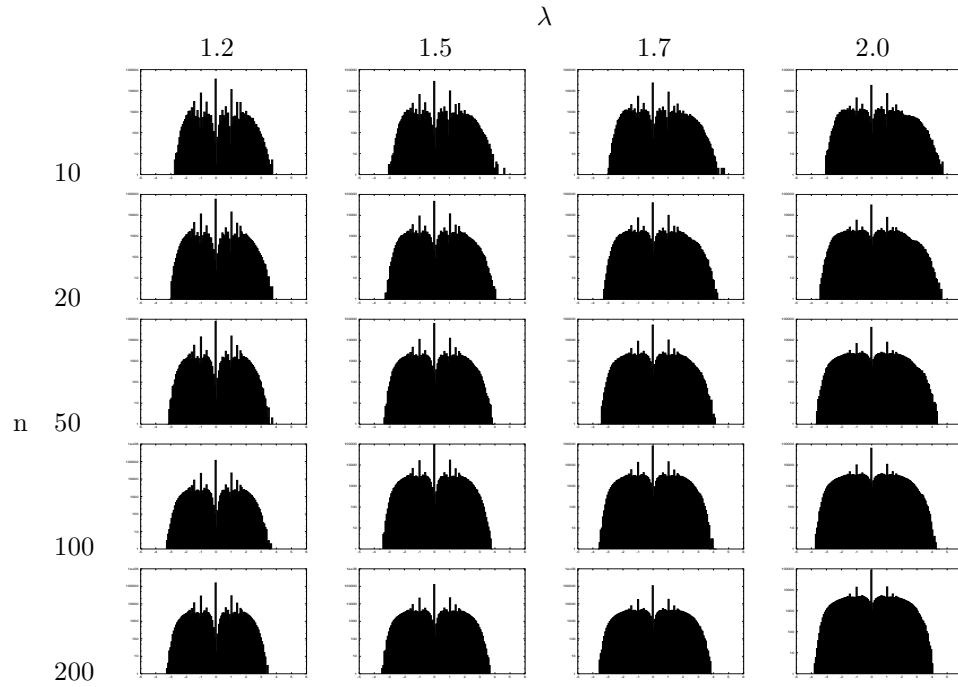


FIGURE 4. Approximations of spectra of sparse matrices for selected  $(\lambda, n)$ ,  $\lambda > 1$ . The axes are as in Figure 1.

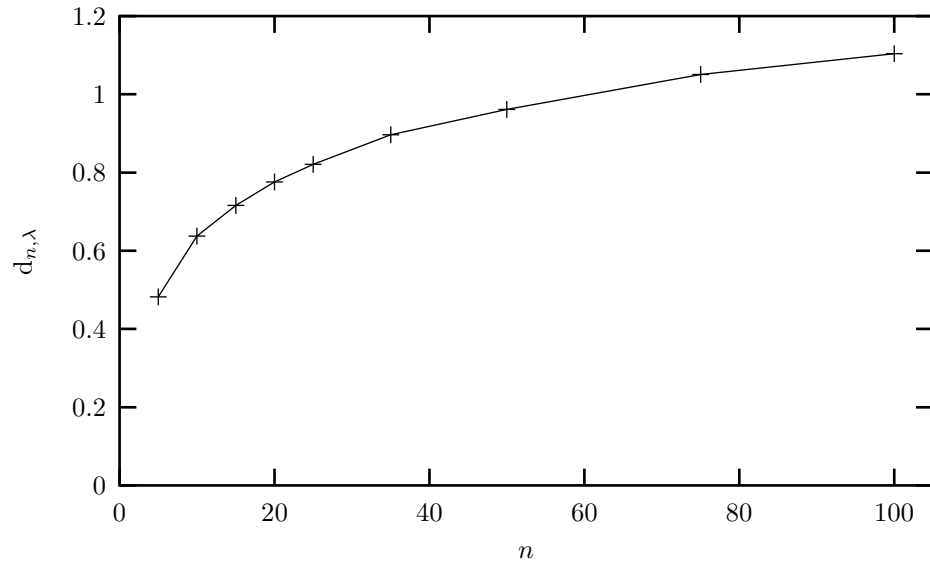


FIGURE 5. Growth of  $d_{\lambda, n}$  in symmetric matrices with normalized Gaussian entries for various values of  $\lambda$ .

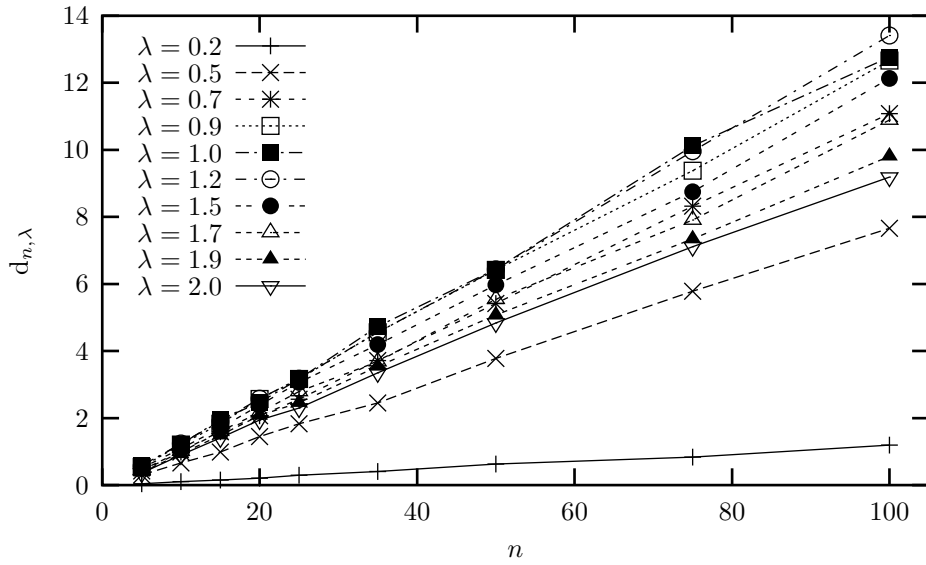


FIGURE 6. Growth of  $d_{\lambda,n}$  in sparse matrices for various values of  $\lambda$ .

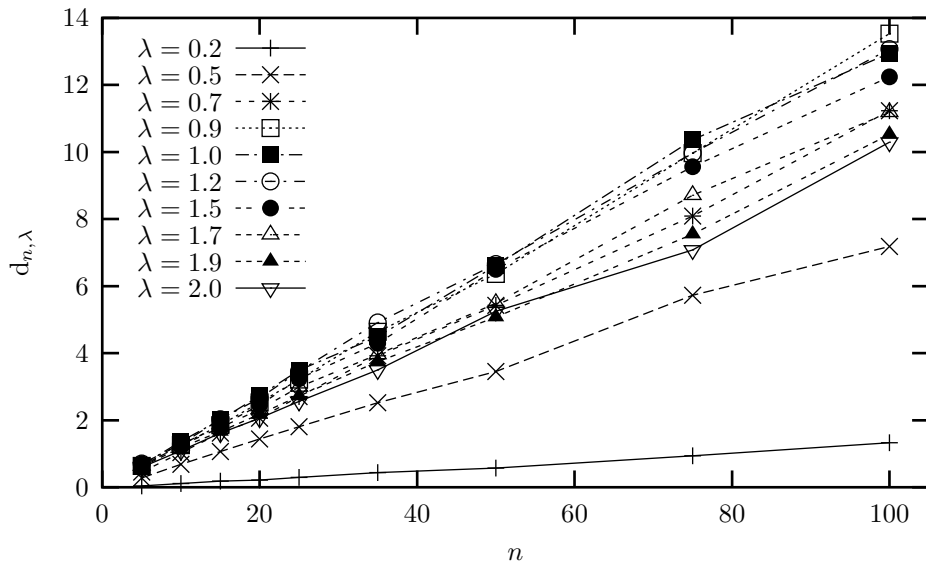


FIGURE 7. Growth of  $d_{\lambda,n}$  in  $\pm$ -sparse matrices for various values of  $\lambda$ .

- (2) All indices identical; there are  $n$  such cases, each yielding  $\langle a_{ij} a_{jk} a_{ki} \rangle = \frac{\lambda}{n}$ , the contribution also going to 0 with  $n \rightarrow \infty$ .
- (3) Two of the indices identical: there are three choices — either  $i = j$ ,  $i = k$  or  $j = k$ . For each, there are  $n(n-1)$  cases. All three yield an expectation of  $(\frac{\lambda}{n})^2$ , so the contribution goes to 0.

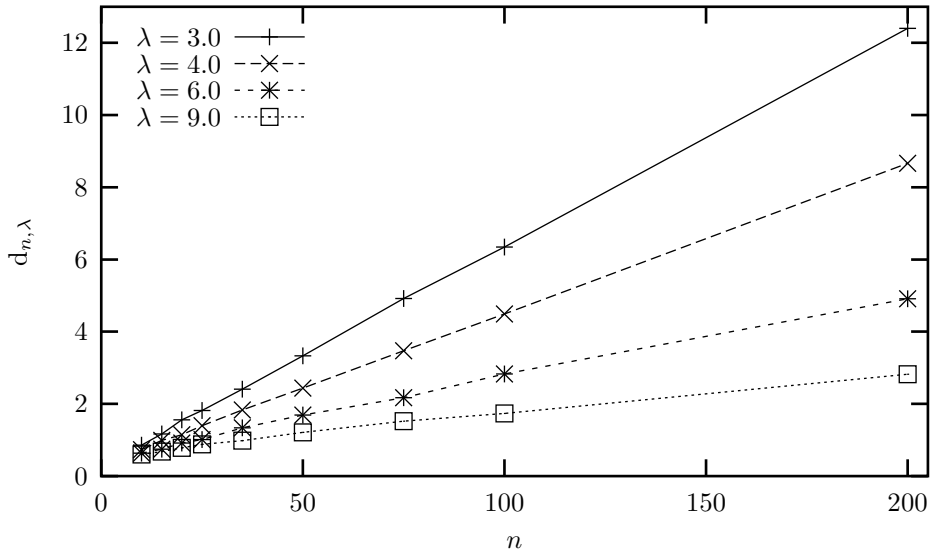


FIGURE 8. Evidence of sublinear growth of  $d_{\lambda,n}$  in  $\pm$ -sparse matrices for higher values of  $\lambda$ .

Hence,  $\lim_{n \rightarrow \infty} \frac{1}{n} \langle \text{Tr } A^3 \rangle = 0$ .

For the next few moments, we performed simple computational estimates:

$$(5) \quad \lim_{n \rightarrow \infty} \frac{1}{n} \langle \text{Tr } A^4 \rangle = \lambda$$

$$(6) \quad \lim_{n \rightarrow \infty} \frac{1}{n} \langle \text{Tr } A^5 \rangle = 0$$

$$(7) \quad \lim_{n \rightarrow \infty} \frac{1}{n} \langle \text{Tr } A^6 \rangle = 12\lambda$$

$$(8) \quad \lim_{n \rightarrow \infty} \frac{1}{n} \langle \text{Tr } A^7 \rangle = 0$$

Since we used a trivial, inefficient approach, for the 8th moment, we only have an estimate:  $50 < \lim_{n \rightarrow \infty} \frac{1}{n} \langle \text{Tr } A^7 \rangle < 60$ .

From what we observed in the spectral estimates (approaching symmetry with  $n \rightarrow \infty$ ), as well as from these estimates of moments, we conjecture that for both sparse and  $\pm$ -sparse matrices all the odd moments are 0.

#### 4. CONCLUSION

Although we have we have no precise results of interest, we present a number of exciting numerical estimates, which suggest a number of further directions of research: is it possible to provide exact descriptions of the linear and sublinear growth patterns? Can we find the limiting spectral densities? How exactly are the discrete eigenvalues of low- $\lambda$  matrices distributed; what are their origins?

#### REFERENCES

- [1] O. Costin and J. L. Lebowitz *Gaussian Fluctuations in Random Matrices*, Phys. Rev. Lett. **75**, 69-72 (1995).



- [2] Intel Corporation, *Intel (R) Math Kernel Library Reference Manual*, Document Number: 630813-011, World Wide Web: <http://developer.intel.com> (2001)
- [3] G. J. Costin and A. J. Bray *Density of states of a sparse random matrix*, Phys. Rev. B **37**, 3557-3562 (1988).